# Communication

## Decoupling and Cloaking of Interleaved Phased Antenna Arrays Using Elliptical Metasurfaces

Hossein Mehrpour Bernety, *Student Member, IEEE*, Alexander B. Yakovlev, *Senior Member, IEEE*, Harry G. Skinner, *Member, IEEE*, Seong-Youp Suh, *Senior Member, IEEE*, and Andrea Alù, *Fellow, IEEE*

***Abstract*— We apply the concept of electromagnetic invisibility/cloaking to improve the radiation properties and decouple two tightly spaced and interleaved phased linear antenna arrays of strip monopoles operating at close frequencies, in order to restore their isolated radiation patterns and eliminate the undesired cross-coupling between their elements. We realize this effect using elliptically shaped cloaking metasurfaces designed for mutually cross-coupled elements of the distinct arrays. We analyze and investigate the cloaking and decoupling effects in improving the functionality of the coupled arrays in terms of their radiation patterns and realized gain, respectively. As a result, the antenna arrays placed in close proximity of each other can radiate independently for a wide range of beam scanning angles, restoring the properties they would have when isolated from each other.**

***Index Terms*— Antenna array, decoupled arrays, elliptical metasurface cloak, mantle cloaking, reduction of mutual coupling.**

### I. Introduction

Recently, the concept of mantle cloaking has been proposed to reduce the scattering cross section of various objects at microwave [1]–[9] and low-terahertz frequencies [10], [11]. Later on, it has been extended to elliptical cylinders and 2-D metallic strips (as special cases) [12]. In [13], it has been proposed to use metamaterials for the reduction of mutual coupling between closely spaced antennas operating at near frequencies. In fact, it is well-known that the mutual interaction between closely spaced antennas degrades antenna performance [14]–[18]. In this regard, the mantle cloaking method has been used for suppressing undesired mutual interactions in antenna applications [19], [20]. Metasurfaces can produce a cloaking effect, which helps restoring the radiation of antennas if blocked by passive elements (by covering those elements with tailored metasurfaces) [21]. Also, an antenna can be cloaked, in such a way that its radar cross section (RCS) is reduced [22].

In many applications, not only the antennas are required to be closely spaced, but also they need to operate at neighboring frequencies. Accordingly, it is desired to simultaneously *decouple* them and *restore their original radiation patterns* as if they were isolated. In this regard, in [23], this concept has been realized using low-profile metasurfaces for two dipole antennas operating at 3.07 and 3.33 GHz with a very small distance equal to one-tenth of the wavelength at 3 GHz. Later on, inspired by the mantle cloaking of elliptical cylinders, in [8] and [12], the concept of simultaneously cloaking and decoupling antennas has been extended to free-standing strip dipoles operating at neighboring frequencies and also two strip dipoles operating at 1 and 5 GHz [24]. In [25] and [26], this concept has been experimentally verified for two single-band monopoles and two single-band and dual-band monopole antennas. In [27], it has been experimentally verified for two monopoles operating at long-term evolution (LTE) and universal mobile telecommunications service (UMTS) bands. It has also been extended to planar microstrip monopoles [28] in printed technology at microwave frequencies and also free-standing strip dipoles at low-THz frequencies [29]. The concept of decoupling and cloaking two printed monopoles, presented in [28], has been experimentally verified in [30]. Very recently, following the procedure in [28], it has also been applied to wideband microstrip monopoles at microwave frequencies [31].

Phased antenna arrays have been used for beam steering in military and industry applications [32]. In conventional antenna arrays, elements are spaced with a distance slightly smaller than half-wavelength to avoid grating lobes [33]. It is of great interest to accommodate compact antenna arrays for various applications, such as multiple-input multiple-output (MIMO) systems, radar detection, mobile communications, among others. However, designing multiple arrays in a fixed area with a small separation between array elements is a challenging problem [34]. In addition, the radiation pattern of an array element is affected by the presence of other elements of the same array (for one array) or elements from other arrays spaced closely (in a multiple-array platform). The main contribution of this article is to address these issues, extending the concepts of cloaking and decoupling based on metasurfaces to phased arrays.

In this article, we show how two closely spaced, interleaved phased antenna arrays, namely, Array I and Array II, which are supposed to operate at neighboring frequencies (not the same), can be *decoupled* from each other and, at the same time, their beam patterns can be *restored* as if they were two isolated arrays. The idea is based on the decoupling and cloaking of two closely spaced strip dipole antennas operating at neighboring frequencies presented in [24]. It should be mentioned that this operation is different from the scenarios considered in [35] and [36], wherein the elements of the same array operating at the same frequency are decoupled. As a result, the length of a linear array will be cut almost in half (in the case of conventional half-wavelength spacing), which may lead to large cost reduction in practical applications and that can be installed on platforms

Manuscript received July 24, 2019; revised October 31, 2019; accepted November 5, 2019. Date of publication December 9, 2019; date of current version June 2, 2020. This work was supported in part by the NSF Industry-University Cooperative Research Centers (I-UCRC) under Grant 1822104 and in part by the Intel Corporation. *(Corresponding author: Hossein Mehrpour Bernety.)*

H. M. Bernety is with the Department of Electrical and Computer Engineering, University of Utah, Salt Lake City, UT 84112 USA (e-mail: hossein.mehrpourbernety@utah.edu).

A. B. Yakovlev is with the Department of Electrical Engineering, University of Mississippi, University, MS 38677-1848 USA (e-mail: yakovlev@olemiss.edu).

H. G. Skinner and S.-Y. Suh are with Intel Corporation, Hillsboro, OR 97124 USA (e-mail: harry.g.skinner@intel.com; seong-youp.suh@intel.com).

A. Alù is with the Advanced Science Research Center, City University of New York, New York, NY 10031 USA (e-mail: aalu@gc.cuny.edu).

Color versions of one or more of the figures in this communication are available online at http://ieeexplore.ieee.org.

Digital Object Identifier 10.1109/TAP.2019.2957286

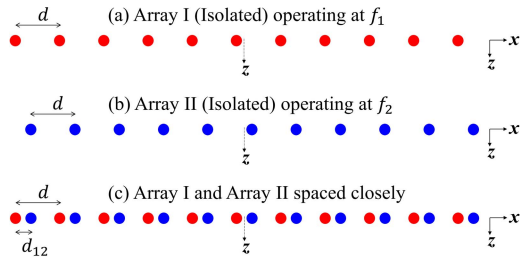


Fig. 1. Isolated (a) Array I operating at $f_1$ and (b) Array II operating at $f_2$. (c) Closely spaced Arrays I and II.

with compact space such as onboard ships, aircrafts, vehicles, etc., and, at the same time, enables frequency diversity. We analyze and investigate how suitably designed metasurfaces covering the antenna elements enable to decouple the two interleaved arrays whether they are phased sequentially (one array is ON, and the other array is OFF) or simultaneously, wherein both arrays are ON and steering the beam toward their respective desired point in space.

This article is organized as follows. In Section II, we provide an analysis of cross-coupling in two closely spaced arrays that are supposed to operate at neighboring frequencies. In Section III, we leverage the concept of mantle cloaking with a metasurface to decouple and cloak two closely spaced, interleaved beam scanning arrays operating at neighboring frequency bands. Section IV is allocated to the conclusion.

## II. Theoretical Analysis of Cross-Coupling

Here, we investigate the effect of cross-coupling between two closely spaced phased antenna arrays that are supposed to operate at neighboring frequencies. In general, the realized gain of an array at frequency $f$ can be written as

$$G_{re}(\theta,\varphi,f)=\frac{e_{\text{tot}}[4\pi U(\theta,\varphi,f)]}{\int_0^{\pi}\int_0^{2\pi} U(\theta,\varphi,f)\sin\theta d\theta d\varphi}\propto e_{\text{tot}}U(\theta,\varphi,f) \quad (1)$$

where $e_{\text{tot}}$ is the total efficiency of the array and $U(\theta,\varphi,f)$ is the radiation intensity.

### A. Cross-Coupled Interleaved Arrays (Sequential Phasing)

Consider now the case in which Array I and Array II are closely spaced, or even interleaved, as shown in Fig. 1(c). We also assume that the arrays are phased sequentially or, in other words, either Array I is ON operating at $f_1$ and Array II is OFF, or Array I is OFF and Array II is ON operating at $f_2$. Let us focus on the case when Array I is ON and Array II is OFF. Due to the presence of the neighboring elements of Array II, the radiation pattern, matching properties and, accordingly, the total efficiency of Array I will change. This deteriorates the constructive far-field coupling (array gain) and significantly reduces the total efficiency. Here, we explore how to minimize this effect, in such a way that the interleaved arrays operate independently of each other, as if they were isolated.

The well-known active element pattern (AEP) technique [37] is commonly used for the analysis of mutual coupling between elements of the same array, but not between two distinct arrays. Ostensibly, it implies that the AEP may not be useful for the analysis of coupling between the elements of two interleaved arrays in our specific problem here. However, here we show that, for the case of two close frequencies of operation, and assuming that the elements of the two arrays have similar free-space radiation patterns

$$\mathbf{F}_{\text{I}}^{fs}(f_1)=\mathbf{F}_{\text{II}}^{fs}(f_1) \quad (2a)$$
$$\mathbf{H}_{\text{I}}^{fs}(f_1)=\mathbf{H}_{\text{II}}^{fs}(f_1) \quad (2b)$$

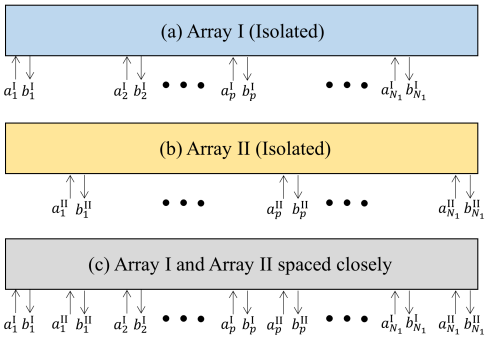


Fig. 2. Multiport network model of isolated (a) Array I and (b) Array II. (c) Closely spaced Arrays I and II.

we can still apply the AEP technique. Here, $\mathbf{F}_{\text{I}}^{fs}(f_1)$ and $\mathbf{F}_{\text{II}}^{fs}(f_1)$ are the free-space vector electric far-field patterns of an element in the Arrays I and II at $f_1$, respectively. Also, $\mathbf{H}_{\text{I}}^{fs}(f_1)$ and $\mathbf{H}_{\text{II}}^{fs}(f_1)$ are the free-space vector magnetic far-field patterns of an element in the Arrays I and II at $f_1$, respectively. Then, the scattering matrix of the whole system (assumed as a multiport network schematically shown in Fig. 2) of two coupled arrays at $f_1$ can be obtained

$$\mathbf{S}(f_1)=\begin{bmatrix}\begin{pmatrix}S_{11}^{\text{I,I}} & \cdots & S_{1N_1}^{\text{I,I}}\\ \vdots & \ddots & \vdots\\ S_{N_11}^{\text{I,I}} & \cdots & S_{N_1N_1}^{\text{I,I}}\end{pmatrix} & \begin{pmatrix}S_{11}^{\text{I,II}} & \cdots & S_{1N_1}^{\text{I,II}}\\ \vdots & \ddots & \vdots\\ S_{N_11}^{\text{I,II}} & \cdots & S_{N_1N_1}^{\text{I,II}}\end{pmatrix}\\ \begin{pmatrix}S_{11}^{\text{II,I}} & \cdots & S_{1N_1}^{\text{II,I}}\\ \vdots & \ddots & \vdots\\ S_{N_11}^{\text{II,I}} & \cdots & S_{N_1N_1}^{\text{II,I}}\end{pmatrix} & \begin{pmatrix}S_{11}^{\text{II,II}} & \cdots & S_{1N_1}^{\text{II,II}}\\ \vdots & \ddots & \vdots\\ S_{N_11}^{\text{II,II}} & \cdots & S_{N_1N_1}^{\text{II,II}}\end{pmatrix}\end{bmatrix}. \quad (3)$$

Accordingly, assuming Array I is ON and Array II is OFF ($a_p^{\text{II}}=0$), the active S-parameter for each element (the $p$th element) of Array I can then be defined as

$$S_p^{\text{I,seq}}(f_1)=\frac{b_p^{\text{I,seq}}(f_1)}{a_p^{\text{I}}}=\frac{1}{a_p^{\text{I}}}\sum_{q=1}^{N_1}a_q^{\text{I}}S_{pq}^{\text{I,I}}(f_1). \quad (4)$$

Here, $a_p^{\text{I}}$ are the complex voltage excitations of the elements of Array I (see Fig. 2). Assuming that it is the same for all elements in Array I ($S_p^{\text{I,seq}}=S_{\text{I}}^{\text{seq}}$), one can also find the total efficiency of Array I due to the presence of Array II

$$e_{\text{tot}}^{\text{I,seq}}(f_1)=1-\left|S_{\text{I}}^{\text{seq}}(f_1)\right|^2. \quad (5)$$

Then, the vector electric and magnetic far-field patterns for an element of Array I can be obtained

$$\mathbf{F}_p^{\text{I,seq}}(f_1)=a_p^{\text{I}}\left[1+S_{\text{I}}^{\text{seq}}(f_1)\right]\mathbf{F}_{\text{I}}^{fs}(f_1) \quad (6a)$$
$$\mathbf{H}_p^{\text{I,seq}}(f_1)=a_p^{\text{I}}\left[1-S_{\text{I}}^{\text{seq}}(f_1)\right]\mathbf{H}_{\text{I}}^{fs}(f_1). \quad (6b)$$

The excitation voltages and currents of the elements of Array II are zero, and with a similar analysis one finds that for an element of Array II

$$\mathbf{F}_p^{\text{II,seq}}(f_1)=b_p^{\text{II,seq}}(f_1)\mathbf{F}_{\text{I}}^{fs}(f_1) \quad (7a)$$
$$\mathbf{H}_p^{\text{II,seq}}(f_1)=-b_p^{\text{II,seq}}(f_1)\mathbf{H}_{\text{I}}^{fs}(f_1) \quad (7b)$$

where

$$b_p^{\text{II,seq}}(f_1)=\sum_{q=1}^{N_1}a_q^{\text{I}}S_{pq}^{\text{II,I}}(f_1). \quad (7c)$$

Then, the total vector electric and magnetic far fields of Array I in the presence of the unexcited elements of Array II, normalized with respect to $e^{-j\beta_1 r}/r$, are obtained as follows:

$$\mathbf{E}_{\text{tot}}^{\text{I,seq}} = \mathbf{F}_{\text{I}}^{fs}(f_1)\left\{\left[1+S_{\text{I}}^{\text{seq}}(f_1)\right]\sum_{p=1}^{N_1} a_p^{\text{I}} e^{j\beta_1(x_p^{\text{I}}\sin\theta\cos\varphi)} + \sum_{p=1}^{N_1} b_p^{\text{II,seq}}(f_1) e^{j\beta_1(x_p^{\text{II}}\sin\theta\cos\varphi)}\right\} \quad (8a)$$

$$\mathbf{H}_{\text{tot}}^{\text{I,seq}} = \mathbf{H}_{\text{I}}^{fs}(f_1)\left\{\left[1-S_{\text{I}}^{\text{seq}}(f_1)\right]\sum_{p=1}^{N_1} a_p^{\text{I}} e^{j\beta_1(x_p^{\text{I}}\sin\theta\cos\varphi)} - \sum_{p=1}^{N_1} b_p^{\text{II,seq}}(f_1) e^{j\beta_1(x_p^{\text{II}}\sin\theta\cos\varphi)}\right\} \quad (8b)$$

where $\beta_1$ is the wavenumber in free space at $f_1$, and $x_p^{\text{I}}$ and $x_p^{\text{II}}$ are the locations of array elements on the $x-$axis [see Fig. 1(c)]. The realized gain pattern of Array I due to this spatial interference will be proportional to

$$G_{re}^{\text{I,seq}}(f_1) \propto e_{\text{tot}}^{\text{I,seq}}(f_1)\text{Re}\{\mathbf{E}_{\text{tot}}^{\text{I,seq}}(f_1)\times\mathbf{H}_{\text{tot}}^{\text{I,seq}^*}(f_1)\}. \quad (9)$$

In the case of a small distance between a pair of neighboring elements belonging to two interleaved arrays:

1) The reflected voltage at the port of an element in Array I is affected by the scattered waves from its closest neighboring element of Array II, and will be different from the isolated case

$$\begin{cases} S_{pp}^{\text{I,I}}(f_1) \neq S_{pp}^{\text{I,iso}}(f_1) \\ S_{pq}^{\text{I,I}}(f_1) \neq S_{pq}^{\text{I,iso}}(f_1) \end{cases} \xrightarrow{\text{yields}} S_{\text{I}}^{\text{seq}}(f_1) \neq S_{\text{I}}^{\text{iso}}(f_1). \quad (10a)$$

Here, $S_{\text{I}}^{\text{iso}}(f_1)$ is the active S-parameter of the isolated Array I [see Fig. 2(a)] at $f_1$ defined in [37], assuming that it is the same for all the elements in Array I ($S_p^{\text{I,iso}} = S_{\text{I}}^{\text{iso}}$).

2) The reflected voltage at the port of an element in Array II is mainly affected by the radiation from its closest neighboring element of Array I. Then, we have

$$b_p^{\text{II,seq}}(f_1) \approx a_p^{\text{I}} S_{pp}^{\text{II,I}}(f_1). \quad (10b)$$

Ideally, we would like that the elements of the interleaved arrays are decoupled from each other, and also that their radiation patterns are similar to the isolated case. To resolve this issue, tailored cloaking metasurfaces wrapped around the distinct array elements can restore the radiation patterns and also decouple two strongly coupled closely spaced antennas operating at neighboring frequencies (with the results shown in Section III). As a result, if an element in Array II is invisible to its closest neighboring element from Array I at frequency $f_1$, we have

$$S_{\text{I}}^{\text{seq}}(f_1) \approx S_{\text{I}}^{\text{iso}}(f_1). \quad (11)$$

In addition, by making the elements of Array II poor radiators (open circuit) at the operation frequency of Array I ($f_1$), such that $b_p^{\text{II,seq}}(f_1) \approx 0$, one can eliminate the undesired cross-coupling between the arrays, and Array I will be operating independently in the presence of Array II, as if it is isolated

$$\mathbf{S}(f_1) = \begin{bmatrix} \begin{pmatrix} S_{11}^{\text{I,iso}} & \cdots & S_{1N_1}^{\text{I,iso}} \\ \vdots & \ddots & \vdots \\ S_{N_1 1}^{\text{I,iso}} & \cdots & S_{N_1 N_1}^{\text{I,iso}} \end{pmatrix} & \begin{pmatrix} 0 & \cdots & 0 \\ \vdots & \ddots & \vdots \\ 0 & \cdots & 0 \end{pmatrix} \\ \begin{pmatrix} 0 & \cdots & 0 \\ \vdots & \ddots & \vdots \\ 0 & \cdots & 0 \end{pmatrix} & \begin{pmatrix} S_{11}^{\text{II,iso}} & \cdots & S_{1N_1}^{\text{II,iso}} \\ \vdots & \ddots & \vdots \\ S_{N_1 1}^{\text{II,iso}} & \cdots & S_{N_1 N_1}^{\text{II,iso}} \end{pmatrix} \end{bmatrix}. \quad (12)$$

### B. Cross-Coupled Interleaved Arrays (Simultaneous Phasing)

Now, we assume that Array I and Array II are closely spaced, as shown in Fig. 1(c), and also, Array I is designed to operate at $f_1$, and Array II is designed to operate at $f_2$. If the elements of Array I and Array II are narrowband, in such a way that there is no overlap in the emitted frequencies, the realized gain patterns of the arrays will be similar to the ones in Section II-A. However, if the operation frequency band of Array II overlaps with $f_1$, then the resulting pattern of Array I at $f_1$ will be the superposition of its own pattern and the pattern of Array II at $f_1$. With a similar analysis to Section II-A, one finds the active S-parameter for each element of Array I can then be defined as

$$S_p^{\text{I,sim}}(f_1) = S_p^{\text{I,seq}}(f_1) + \frac{1}{a_p^{\text{I}}}\sum_{q=1}^{N_1} a_q^{\text{II}} S_{pq}^{\text{I,II}}(f_1). \quad (13)$$

Assuming that this is the same for all elements in Array I ($S_p^{\text{I,sim}} = S_{\text{I}}^{\text{sim}}$), one can also find the total efficiency of Array I when Array II is ON as

$$e_{\text{tot}}^{\text{I,sim}}(f_1) = 1 - \left|S_{\text{I}}^{\text{sim}}(f_1)\right|^2. \quad (14)$$

Similarly, the active S-parameter for each element of Array II and its total efficiency will be

$$S_p^{\text{II,sim}}(f_1) = \frac{b_p^{\text{II,seq}}(f_1)}{a_p^{\text{II}}} + \frac{1}{a_p^{\text{II}}}\sum_{q=1}^{N_1} a_q^{\text{I}} S_{pq}^{\text{II,I}}(f_1). \quad (15)$$

Hence, the realized gain pattern of Array I at $f_1$ in the presence of Array II will be proportional to

$$G_{re}^{\text{I,sim}}(\theta,\varphi,f_1) \propto e_{\text{tot}}^{\text{I,sim}}(f_1)\text{Re}\left[\mathbf{E}_{\text{tot}}^{\text{I,sim}}(f_1)\times\mathbf{H}_{\text{tot}}^{\text{I,sim*}}(f_1)\right] \approx e_{\text{tot}}^{\text{I,sim}}(f_1)\left\|\mathbf{F}_{\text{I}}^{fs}(f_1)\right\|^2 g_{re}^{\text{I,sim}}(f_1) \quad (16)$$

where $g_{re}^{\text{I,sim}}(f_1)$ is the normalized gain pattern, and assuming uniform excitations for both arrays we obtain

$$g_{re}^{\text{I,sim}}\left(f_1, |a_p^{\text{I}}| = |a_p^{\text{II}}| = 1\right) = \left|\sqrt{e_{\text{tot}}^{\text{I,sim}}(f_1)}\sum_{p=1}^{N_1} e^{j\delta_p^{\text{I}}} e^{j\beta_1(x_p^{\text{I}}\sin\theta\cos\varphi)} + \sqrt{e_{\text{tot}}^{\text{II,sim}}(f_1)}\sum_{p=1}^{N_1} e^{j\delta_p^{\text{II}}} e^{j\beta_1(x_p^{\text{II}}\sin\theta\cos\varphi)}\right|^2. \quad (17)$$

Here $\delta_p^{\text{I}}$ and $\delta_p^{\text{II}}$ are the excitation phases of the elements of Array I and Array II, respectively.

Now, considering Fig. 1(c), we investigate how the electromagnetic interference between the arrays changes the normalized realized gain pattern of Array I with two examples. First, we assume that the 11 elements of Array I are fed with a phase pattern aimed at steering the beam toward $\theta_0 = 30^\circ$ at the center frequency $f_1 = 2.95$ GHz, and the 11 elements of Array II are fed to steer the beam toward

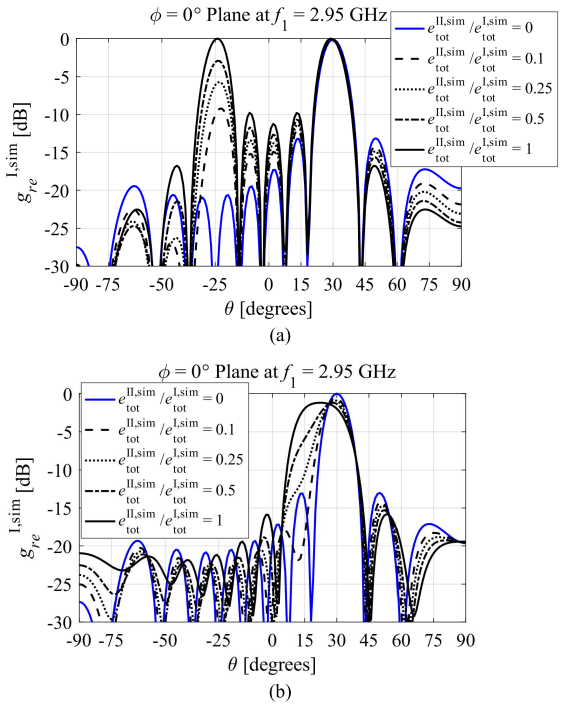


Fig. 3. Normalized realized gain pattern of Array I at 2.95 GHz when Array II is also ON at $f_1 = 2.95$ GHz for different values of the total efficiency ratio. (a) Array I with $\theta_0 = 30°$ and Array II with $\theta_0 = -25°$. (b) Array I with $\theta_0 = 30°$ and Array II with $\theta_0 = 15°$.

$\theta_0 = -25°$ at the center frequency $f_2 = 3.35$ GHz. The distance values are $d = 50$ mm and $d_{12} = 10$ mm. The analysis below concerns the case when the operation frequency band of Array II overlaps with the frequency $f_1$ (even though the Array II was designed to operate at the center frequency $f_2$). In this regard, we excite both arrays at $f_1$, as the center frequency of Array I. According to the superposition principle, the gain of Array I will be affected by Array II. This superposition is a function of the total efficiency of Array II at the frequency $f_1$. To quantitatively investigate this effect, the results for the normalized realized gain pattern of Array I [given by (17)] in dB are shown in Fig. 3(a) for various values of the ratio of the total efficiencies ($e^{II,sim}_{tot}/e^{I,sim}_{tot}$) at $f_1$. It can be seen that high interference (large ratio) may lead to large side lobes for the Array I, due to the superposition of its own pattern and the pattern of Array II at $f_1$. Then, we assume the elements of Array I and Array II are designed to steer the beam toward $\theta_0 = 30°$ at the center frequency $f_1 = 2.95$ GHz and $\theta_0 = 15°$ at the center frequency $f_2 = 3.35$ GHz, respectively. Again, we excite both arrays at $f_1$. The results are shown in Fig. 3(b). In this case, not only the main beam of Array I shifts, but also its shape will be deformed in the case of high interference between the arrays.

It can be concluded that the cloak metasurfaces, wrapped around the elements of Array II, not only should make these elements invisible to the elements of Array I at $f_1$ (and vice versa at $f_2$) due to the cloaking effect but also should make these elements poor radiators with a low total efficiency at $f_1$ (and vice versa at $f_2$) by decoupling the arrays and minimizing the ratio of the total efficiencies. In Section III, we show how this objective can be achieved.

## III. Decoupling and Cloaking of Interleaved Phased Antenna Arrays

Now, we consider two closely spaced (interleaved) linear antenna arrays, namely, Array I and Array II (schematically shown in Fig. 4),

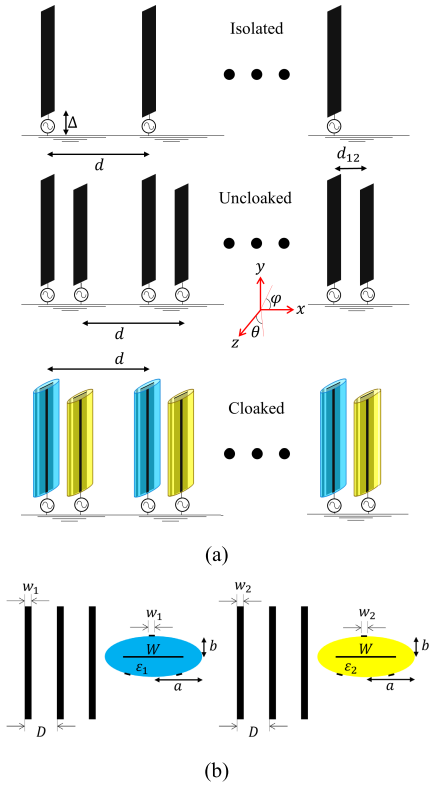


Fig. 4. (a) Schematics of isolated Array I, uncloaked coupled arrays, and cloaked decoupled arrays. (b) Schematics of the elliptical metasurface cloaks and the cross-section views of Antenna I (left) and Antenna II (right).

TABLE I
Design Parameters of Antenna I and Antenna II

| Antenna I (Isolated or Uncloaked) | Antenna I (Cloaked) | Antenna II (Isolated or Uncloaked) | Antenna II (Cloaked) |
|---|---|---|---|
| $W = 4$ mm | $W = 4$ mm | $W = 4$ mm | $W = 4$ mm |
| - | $a = 2.2$ mm | - | $a = 2.2$ mm |
| - | $b = 0.9165$ mm | - | $b = 0.9165$ mm |
| $L_1 = 22.9$ mm | $L_1 = 20.7$ mm | $L_2 = 20.75$ mm | $L_2 = 19.4$ mm |
| - | $D = 3.4034$ mm | - | $D = 3.4034$ mm |
| - | $w_1 = 0.35$ mm | - | $w_2 = 0.3$ mm |
| - | $\varepsilon_1 = 6.15$ | - | $\varepsilon_2 = 9.8$ |
| $\Delta = 0.1$ mm | $\Delta = 0.1$ mm | $\Delta = 0.1$ mm | $\Delta = 0.1$ mm |

supposed to be operating at $f_1 = 2.95$ GHz and $f_2 = 3.35$ GHz, respectively, each with $N = 11$ elements located on the $x-$axis. The spacing for each array is $d = 50$ mm (which is $\lambda_1/2$ or $0.56\lambda_2$), and the inter-element spacing between the two arrays is $d_{12} = 10$ mm (which is $\lambda_1/10.2$ or $\lambda_2/9$). From array theory (considering the array factor of a linear array) [32], in our example, the scan angle ranges are $-90° \le \theta_0^{I} \le 90°$ and $-50° \le \theta_0^{II} \le 50°$, for Arrays I and II, respectively. To illustrate the concept of restoring array beam scanning and gain properties using cloaking metasurfaces, we assume three different cases: 1) the arrays operate independently of each other (isolated); 2) the arrays are closely spaced, coupled, but uncloaked; and 3) the arrays are closely spaced, decoupled and cloaked by the elliptical metasurface cloaks, as shown in Fig. 4(a).

Here, we consider the array elements made of strip monopole antennas (i.e., Antenna I and Antenna II) excited by 37.5 Ω discrete ports, vertically positioned with respect to an infinite ground plane. The various parameters of the two monopole antennas and their respective metasurfaces [shown in Fig. 4(b)] have been found using

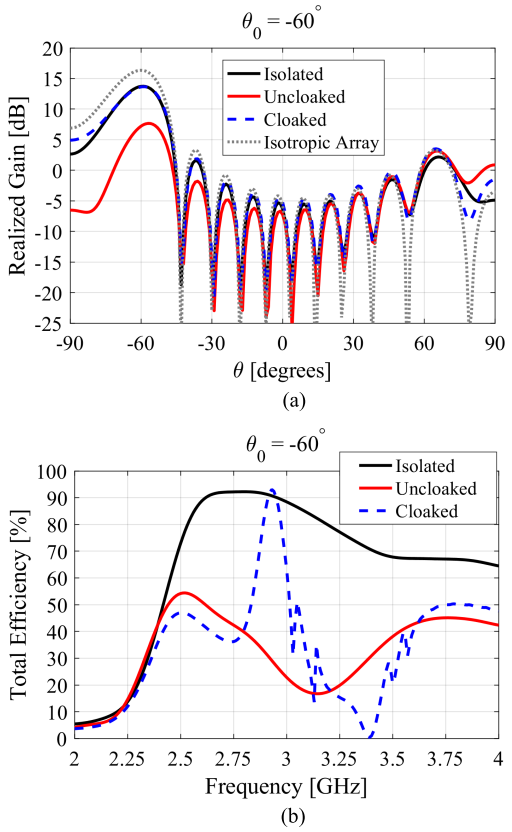


Fig. 5. (a) Realized gain at $f_1 = 2.95$ GHz. (b) Total efficiency of Array I for $\theta_0 = -60°$.

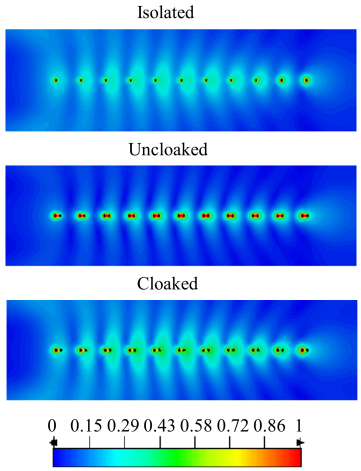


Fig. 6. Normalized electric field distribution of Array I for $\theta_0 = -60°$ at $f_1 = 2.95$ GHz for isolated, uncloaked coupled, and cloaked decoupled cases.

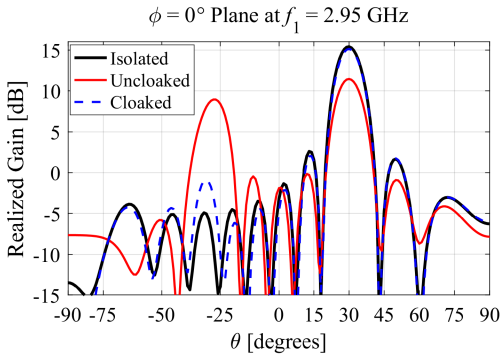


Fig. 7. Realized gain patterns of Array I with $\theta_0 = 30°$ at $f_1 = 2.95$ GHz, when Array II is simultaneously excited at $f_1$.

the design procedure in [24] for strip dipoles, as given in Table I. In fact, once the optimization is done for dipoles, the same parameters can also be used for their equivalent strip monopole antennas, and should still work in the presence of an array of antennas, since the cloak performance should not be affected by the environment, even in the near field [38]. The corresponding simulations have been performed using CST MWS [39].

### A. *Sequential Phasing (Array I is* ON *and Array II is* OFF*)*

In this scenario, we investigate the effect of using metasurfaces when each element of Array I is excited and the elements of Array II are OFF. A similar analysis has been performed when Array I is OFF and Array II is ON, but it is not shown here for the sake of brevity.

Here, we provide the realized gain of Array I for the three scenarios of Fig. 4(a). For the sake of brevity, we have chosen the scan angle of $\theta_0 = -60°$ and its respective realized gain is shown in Fig. 5(a). It can be seen that the elliptical metasurface cloaks, wrapped around the elements of Array II, provide restoration of the patterns of Array I in the presence of Array II, despite the small spacing. Also, Fig. 5(b) shows the total efficiency of Array I, wherein the elliptical metasurface cloaks, wrapped around the elements of Array II, make it possible to recover the total efficiency of Array I around $f_1 = 2.95$ GHz, and at the same time, the elliptical metasurface cloaks, wrapped around the elements of Array I, make this array a poor radiator at the resonance frequency of Array II, and thus, *decouples* them. Also, for $\theta_0 = -60°$, here we provide a comparison between the electric field distributions of the isolated, uncloaked coupled, and cloaked decoupled cases as shown in Fig. 6. It can be seen how the metasurface cloaks can restore the field distribution and result in a radiation similar to the isolated case. Also, in Fig. 6 (middle panel), it can be seen that in the case of two coupled (uncloaked) arrays, the Array I is a poor radiator due to its strong cross-coupling with the elements of Array II.

### B. *Simultaneous Phasing (Array I is* ON *and Array II is* ON*)*

Here, we provide simulation results for the case that the interleaved, closely spaced Array I and Array II [see Fig.1(c)] are both ON, each with 11 elements. Array I is designed to operate at the center frequency $f_1 = 2.95$ GHz, and simultaneously, Array II is designed to operate at $f_2 = 3.35$ GHz.

As an example, we assume that the elements of Array I are supposed to steer the beam toward $\theta_0 = 30°$ at the center frequency $f_1 = 2.95$ GHz, and the elements of Array II are phased, in such a way that steer the beam toward $\theta_0 = -25°$ at the center frequency $f_2 = 3.35$ GHz. The analysis below concerns the case when the operation frequency band of Array II overlaps with the frequency $f_1$ (even though the Array II was designed to operate at the center frequency $f_2$). To find the effect of the superposition of patterns for Array I at 2.95 GHz, we excite both arrays at $f_1 = 2.95$ GHz. The distance values are $d = 50$ mm and $d_{12} = 10$ mm. Then, we cover the elements of each array by the proposed metasurface cloaks (described in Section III). The results for the realized gain pattern of Array I at $f_1$ =2.95 GHz in dB are shown in Fig. 7 for the isolated, uncloaked coupled, and cloaked decoupled cases.

The metasurface cloaks wrapped around the elements of Array II make them poor radiators at $f_1$ =2.95 GHz, in such a way that

the ratio of the total efficiency of Array II to that of Array I changes from 0.61 in the uncloaked coupled case to 0.06 in the cloaked decoupled case. Accordingly, they dramatically reduce the large sidelobe (almost 10 dB), occurred due to the superposition of patterns at $f_1$. In addition, these metasurface cloaks make the elements of Array II hidden to the elements of Array I, which improve the desired main beam (almost 4 dB) of Array I, in such a way that Array I functions as in the case when it is isolated. The results confirm the analysis presented in Section II. A similar analysis can be performed for Array II at $f_2 = 3.35$ GHz, not shown here for the sake of brevity.

## IV. Conclusion

In this article, we have proposed to utilize the established mantle cloaking method in order to decouple and cloak two closely spaced and interleaved phased antenna arrays operating at neighboring frequencies, to restore their radiation patterns and recover their matching properties, in such a way that the two distinct arrays operate independently of each other as if they were isolated. We have theoretically analyzed the cross-coupling of such arrays. The presented simulation results confirm our theoretical analysis, and show that decoupling and cloaking of two antennas operating at different but close frequencies can be generalized to two decoupled and cloaked antenna arrays, in a cost-effective and size-reduced manner, leading to densely packed arrays with high efficiency and beam scanning capabilities.

## References


[1] A. Alù, "Mantle cloak: Invisibility induced by a surface," *Phys. Rev. B, Condens. Matter*, vol. 80, no. 24, p. 245115, Dec. 2009.

[2] P.-Y. Chen and A. Alú, "Mantle cloaking using thin patterned metasurfaces," *Phys. Rev. B, Condens. Matter*, vol. 84, no. 20, p. 205110, Nov. 2011.

[3] P.-Y. Chen, F. Monticone, and A. Alu, "Suppressing the electromagnetic scattering with an helical mantle cloak," *IEEE Antennas Wireless Propag. Lett.*, vol. 10, pp. 1598–1601, 2011.

[4] P.-Y. Chen, C. Argyropoulos, and A. Alù, "Broadening the cloaking bandwidth with non-foster metasurfaces," *Phys. Rev. Lett.*, vol. 111, Dec. 2013, Art. no. 233001.

[5] L. Matekovits and T. S. Bird, "Width-modulated microstrip-line based mantle cloaks for thin single- and multiple cylinders," *IEEE Trans. Antennas Propag.*, vol. 62, no. 5, pp. 2606–2615, May 2014.

[6] Y. R. Padooru, A. B. Yakovlev, P. Y. Chen, and A. Alù, "Analytical modeling of conformal mantle cloaks for cylindrical objects using sub-wavelength printed and slotted arrays," *J. Appl. Phys.*, vol. 112, Aug. 2012, Art. no. 0349075.

[7] Y. R. Padooru, A. B. Yakovlev, P.-Y. Chen, and A. Alù, "Line-source excitation of realistic conformal metasurface cloaks," *J. Appl. Phys.*, vol. 112, no. 10, p. 104902, 2012.

[8] H. M. Bernety and A. B. Yakovlev, "Conformal and confocal mantle cloaking of elliptical cylinders using sub-wavelength metallic meshes and patches," in *Proc. IEEE APS Int. Symp.*, Jul. 2014, pp. 1433–1434.

[9] Z. H. Jiang and D. H. Werner, "Exploiting metasurface anisotropy for achieving near-perfect low-profile cloaks beyond the quasi-static limit," *J. Phys. D, Appl. Phys.*, vol. 46, Nov. 2013, Art. no. 505306.

[10] P.-Y. Chen and A. Alù, "Atomically thin surface cloak using graphene monolayers," *ACS Nano*, vol. 5, pp. 5855–5863, Jun. 2011.

[11] P.-Y. Chen, J. Soric, Y. R. Padooru, H. M. Bernety, A. B. Yakovlev, and A. Alù, "Nanostructured graphene metasurface for tunable terahertz cloaking," *New J. Phys.*, vol. 15, pp. 123029-1–123029-12, Dec. 2013.

[12] H. M. Bernety and A. B. Yakovlev, "Cloaking of single and multiple elliptical cylinders and strips with confocal elliptical nanostructured graphene metasurface," *J. Phys., Condens. Matter*, vol. 18, Apr. 2015, Art. no. 185304.

[13] D. H. Kwon and D. H. Werner, "Restoration of antenna parameters in scattering environments using electromagnetic cloaking," *Appl. Phys. Lett.*, vol. 92, no. 11, 2008, Art. no. 113507.

[14] F. Yang and Y. Rahmat-Samii, "Microstrip antennas integrated with electromagnetic band-gap (EBG) structures: A low mutual coupling design for array applications," *IEEE Trans. Antennas Propag.*, vol. 51, no. 10, pp. 2936–2946, Oct. 2003.

[15] C.-Y. Chiu, C.-H. Cheng, R. D. Murch, and C. R. Rowell, "Reduction of mutual coupling between closely-packed antenna elements," *IEEE Trans. Antennas Propag.*, vol. 55, no. 6, pp. 1732–1738, Jun. 2007.

[16] M. A. Khayat, J. T. Williams, D. R. Jackson, and S. A. Long, "Mutual coupling between reduced surface-wave microstrip antennas," *IEEE Trans. Antennas Propag.*, vol. 48, no. 10, pp. 1581–1593, Oct. 2000.

[17] H. S. Farahani, M. Veysi, M. Kamyab, and A. Tadjalli, "Mutual coupling reduction in patch antenna arrays using a UC-EBG superstrate," *IEEE Antennas Wireless Propag. Lett.*, vol. 9, pp. 57–59, 2010.

[18] P. Alitalo, J. Vehmas, and S. A. Tretyakov, "Reduction of antenna blockage with a transmission-line cloak," in *Proc. 5th Eur. Conf. Antennas Propag. (EuCAP)*, Apr. 2011, pp. 2399–2402.

[19] J. C. Soric, A. Monti, A. Toscano, F. Bilotti, and A. Alù, "Dual-polarized reduction of dipole antenna blockage using mantle cloaks," *IEEE Trans. Antennas Propag.*, vol. 63, no. 11, pp. 4827–4834, Nov. 2015.

[20] A. Monti, J. Soric, A. Alù, A. Toscano, and F. Bilotti, "Design of cloaked Yagi-Uda antennas," *EPJ Appl. Metamater.*, vol. 3, no. 10, pp. 1–7, Nov. 2016.

[21] P. Alitalo, C. A. Valagiannopoulos, and S. A. Tretyakov, "Simple cloak for antenna blockage reduction," in *Proc. IEEE Antennas Propag. Soc. Int. Symp.*, Jul. 2011, pp. 669–672.

[22] C. A. Valagiannopoulos and N. L. Tsitsas, "Integral equation analysis of a low-profile receiving planar microstrip antenna with a cloaking superstrate," *Radio Sci.*, vol. 47, pp. 1–2, Apr. 2012.

[23] A. Monti, J. Soric, A. Alù, F. Bilotti, A. Toscano, and L. Vegni, "Overcoming mutual blockage between neighboring dipole antennas using a low-profile patterned metasurface," *IEEE Antennas Wireless Propag. Lett.*, vol. 11, pp. 1414–1417, Dec. 2012.

[24] H. M. Bernety and A. B. Yakovlev, "Reduction of mutual coupling between neighboring strip dipole antennas using confocal elliptical metasurface cloaks," *IEEE Trans. Antennas Propag.*, vol. 63, no. 4, pp. 1554–1563, Apr. 2015.

[25] Z. H. Jiang, P. E. Sieber, L. Kang, and D. H. Werner, "Restoring intrinsic properties of electromagnetic radiators using ultralightweight integrated metasurface cloaks," *Adv. Funct. Mater.*, vol. 25, no. 29, pp. 4708–4716, Aug. 2015.

[26] Z. H. Jiang and D. H. Werner, "Dispersion engineering of metasurfaces for dual-frequency quasi-three-dimensional cloaking of microwave radiators," *Opt. Express*, vol. 24, no. 9, pp. 9629–9644, May 2016.

[27] A. Monti *et al.*, "Mantle cloaking for co-site radio-frequency antennas," *Appl. Phys. Lett.*, vol. 108, no. 11, p. 113502, 2016.

[28] H. M. Bernety and A. B. Yakovlev, "Decoupling antennas in printed technology using elliptical metasurface cloaks," *J. Appl. Phys.*, vol. 119, no. 1, pp. 014904-1–014904-11, Apr. 2016.

[29] G. Moreno, H. M. Bernety, and A. B. Yakovlev, "Reduction of mutual coupling between strip dipole antennas at terahertz frequencies with an elliptically shaped graphene monolayer," *IEEE Antennas Wireless Propag. Lett.*, vol. 15, pp. 1533–1536, Dec. 2015.

[30] G. Gulati, "Novel antennas, matching circuits, and fabrication techniques at HF and microwave frequencies," M.S. thesis, Dept. Elect. Eng., Univ. Arizona, Tucson, AZ, USA, 2018.

[31] G. Moreno *et al.*, "Wideband elliptical metasurface cloaks in printed antenna technology," *IEEE Trans. Antennas Propag.*, vol. 66, no. 7, pp. 3512–3525, Jul. 2018.

[32] D. Parker and D. Z. Zimmermann, "Phased arrays-part 1: Theory and architectures," *IEEE Trans. Microw. Theory Techn.*, vol. 50, no. 3, pp. 678–687, Mar. 2002.

[33] C. A. Balanis, *Antenna Theory: Analysis and Design*, 4th ed. Hoboken, NJ, USA: Wiley, 2016.

[34] M. Stoytchev, H. Safar, A. L. Moustakas, and S. Simon, "Compact antenna arrays for MIMO applications," in *Proc. IEEE Antennas Propag. Soc. Int. Symp.*, Boston, MA, USA, vol. 3, Jul. 2001, pp. 708–711.

[35] Z. Wang *et al.*, "A meta-surface antenna array decoupling (MAAD) method for mutual coupling reduction in a MIMO antenna system," *Sci. Rep.*, vol. 8, no. 1, 2018, Art. no. 3152.

[36] Z. C. Niu, H. Zhang, Q. Chen, and T. Zhong, "Isolation enhancement using a novel array-antenna decoupling surface for microstrip antennas," *Prog. Electromagn. Res. M*, vol. 72, pp. 49–59, Aug. 2018.

[37] D. M. Pozar, "The active element pattern," *IEEE Trans. Antennas Propag.*, vol. 42, no. 8, pp. 1176–1178, Sep. 1994.

[38] A. Alù and N. Engheta, "Cloaking and transparency for collections of particles with metamaterial and plasmonic covers," *Opt. Express*, vol. 15, no. 12, pp. 7578–7590, Jun. 2007.

[39] (2015). *CST Microwave Studio*. [Online]. Available: http://www.cst.com